Molecular Cancer Therapeutics

Chemogenetic Evaluation of the Mitotic Kinesin CENP-E Reveals a Critical Role in Triple-Negative Breast Cancer

Pei-Pei Kung[1], Ricardo Martinez[2], Zhou Zhu[2], Michael Zager[3], Alessandra Blasina[2], Isha Rymer[2], Jill Hallin[2], Meirong Xu[2], Christopher Carroll[2], John Chionis[2], Peter Wells[2], Kirk Kozminski[3], Jeffery Fan[2], Oivin Guicherit[2], Buwen Huang[1], Mei Cui[2], Chaoting Liu[2], Zhongdong Huang[2], Anand Sistla[4], Jennifer Yang[2], and Brion W. Murray[2]

Abstract

Breast cancer patients with tumors lacking the three diagnostic markers (ER, PR, and HER2) are classified as triple-negative (primarily basal-like) and have poor prognosis because there is no disease-specific therapy available. To address this unmet medical need, gene expression analyses using more than a thousand breast cancer samples were conducted, which identified elevated centromere protein E (CENP-E) expression in the basal-a molecular subtype relative to other subtypes. CENP-E, a mitotic kinesin component of the spindle assembly checkpoint, is shown to be induced in basal-a tumor cell lines by the mitotic spindle inhibitor drug docetaxel. CENP-E knockdown by inducible shRNA reduces basal-a breast cancer cell viability. A potent, selective CENP-E inhibitor (PF-2771) was used to define the contribution of CENP-E motor function to basal-like breast cancer. Mechanistic evaluation of PF-2771 in basal-a tumor cells links CENP-E–dependent molecular events (e.g., phosphorylation of histone H3 Ser-10; phospho-HH3-Ser_{10}) to functional outcomes (e.g., chromosomal congression defects). Across a diverse panel of breast cell lines, CENP-E inhibition by PF-2771 selectively inhibits proliferation of basal breast cancer cell lines relative to premalignant ones and its response correlates with the degree of chromosomal instability. Pharmacokinetic–pharmacodynamic efficacy analysis in a basal-a xenograft tumor model shows that PF-2771 exposure is well correlated with increased phospho-HH3-Ser_{10} levels and tumor growth regression. Complete tumor regression is observed in a patient-derived, basal-a breast cancer xenograft tumor model treated with PF-2771. Tumor regression is also observed with PF-2771 in a taxane-resistant basal-a model. Taken together, CENP-E may be an effective therapeutic target for patients with triple-negative/basal-a breast cancer. *Mol Cancer Ther; 13(8); 2104–15. ©2014 AACR.*

Introduction

Breast cancer is many diseases coarsely stratified into distinct patient populations using three immunohistochemistry tumor markers: estrogen receptor (ER), progesterone receptor (PR), and the human epidermal growth factor receptor-2 (HER2/neu, erbB2; refs. 1, 2). The segment that does not express any of these markers (triple-negative breast cancer, TNBC) constitutes 10% to 20% of all patients with breast cancer, often premenopausal women and members of specific ethnic groups such as African decent (3). Genomic analysis has refined the classification of breast cancer with the majority of TNBC tumors classified as basal-like (4). Basal tumor cells are further segmented into basal-a and basal-b (claudin-low). Understanding breast cancer tumor biology has powered dramatic improvements in survival for patients with therapies that target their specific disease biology. ER-positive breast cancer has effective therapies such as ER antagonists (e.g., tamoxifen, FDA-approved in 1977) and estrogen biosynthesis inhibitors (aromatase drugs, FDA-approved in the 1990s). HER2-driven disease has effective therapies: trastuzumab (FDA-approved in 1998), lapatinib (FDA-approved in 2007), pertuzumab (FDA-approved 2012), and kadcyla (FDA-approved 2013). In contrast, "triple-negative" breast has no approved targeted therapies and as a consequence, patient prognosis remains poor (5).

Recent clinical studies suggest that patients with TNBC respond to standard chemotherapy cytotoxic

Authors' Affiliations: [1]Oncology Chemistry, [2]Oncology Research Unit, [3]Pharmacokinetics, Dynamics and Metabolism, and [4]Pharmaceuticals Science, Pfizer Worldwide Research and Development, La Jolla Laboratories, San Diego, California

Note: Supplementary data for this article are available at Molecular Cancer Therapeutics Online (http://mct.aacrjournals.org/).

Current address for R. Martinez: Eli Lilly and Company, Indianapolis, IN; current address for C. Carroll: Arena Pharmaceuticals, Inc., San Diego, CA; current address for Z. Huang: Halozyme Therapeutics Inc., San Diego CA; current address for M. Zager: Johnson & Johnson, San Diego, CA; current address for K. Kozminski: Ferring Research Institute Inc., San Diego, CA; current address for J. Yang: Johnson & Johnson, San Diego, CA.

P.-P. Kung and R. Martinez contributed equally to this article.

Corresponding Author: Brion W. Murray, Pfizer Worldwide Research and Development, La Jolla, Pfizer Inc., 10777 Science Center Drive, San Diego, CA 92121. Phone: 858-622-6038; Fax: 858-526-4240; E-mail: brion.murray@pfizer.com

doi: 10.1158/1535-7163.MCT-14-0083-T

regimens (e.g., taxanes; ref. 6), which are also the backbone to most breast cancer treatments. Taxanes block the microtubule contribution to mitotic spindles, alter chromosomal segregation, block the cell-cycle progression, and therefore inhibit cell proliferation. Unfortunately, the clinical benefit for patients with TNBC is not durable (6). In addition, taxanes are known as spindle poisons because they inhibit functions conserved in normal physiology and cause severe toxicities (e.g., neutropenia, neuropathy; refs. 7, 8) A better approach would be if this process could be selectively modulated in cancer cells. From both efficacy and tolerability perspectives, improved TNBC therapies are needed.

Genomic analysis of a broad array of breast cancer samples identified *CENPE* as a candidate gene for targeting TNBC. CENP-E is a component of the kinetochore complex critical to chromosome congression and alignment in mitosis as part of the spindle assembly checkpoint (SAC, mitotic checkpoint; refs. 9–11). CENP-E uses an ATPase activity (motor function) to slide nonaligned chromosomes along mitotic spindles toward the equatorial plate (metaphase plate) and establish metaphase before chromosome segregation. A potent, specific, small-molecule inhibitor of CENP-E motor function (PF-2771) was synthesized and used to characterize the CENP-E motor function in tumor cells and models. These studies provide support for a significant role of CENP-E in the basal-a/TNBC.

Materials and Methods

Cell lines

Cell lines described in this work were obtained from ATCC. Cell cultures were expanded by serial passaging and stocks frozen after 3 to 5 passages.

Chromosomal instability index analysis

Chromosomal instability (CIN) index is a measure of deviation from a diploid state (aneuploidy). To quantify the degree of global copy-number change in each cell line (16 lines analyzed), a CIN index was calculated from genome-wide SNP array data by taking into account both the length and amplitude of changes as following:

$$\mathrm{CIN} = \frac{\sum_{i=1}^{L} l_i \times |a_i|}{\sum_{i=1}^{L} l_i},$$

where l_i and a_i are the length and mean amplitude (on $\log_2$ scale) of each copy-number segment, respectively, and L corresponds to total number of segments in the genome (chromosomes 1 to 22 and X). Perfectly diploid cells have a CIN score of zero.

Inducible small hairpin RNA studies

Basal-like breast cancer HCC1806 cells that were engineered with small hairpin RNA (shRNA) constructs were exposed to doxycycline (1 μg/mL) to induce their expression (CENP-E specific, GCAGAGAGTGTGGATTCTCAG; KIF11 shRNA as a positive control; nontargeting, CAACAAGATGAAGAGCACCAA, luciferase shRNA). Purified mRNA (Illustra RNAspin Mini Isolation Kit; GE Healthcare Lifesciences) was converted into cDNA (qScript cDNA SuperMix; Quanta BioSciences) and analyzed by qPCR in triplicate (hydrolysis probes and Master Mix purchased from Applied Biosystems). HCC1806 cell viability was measured after the shRNA induction. Cells were seeded the day before doxycycline addition, incubated with shRNA for 3 days after addition of eight doxycycline concentrations, PBS washed, trypsinized, stained with 0.4% trypan blue (Invitrogen), and counted under microscope.

Biochemical assay of CENP-E enzymatic activity

Microtubule-activated CENP-E kinesin ATPase activity was measured spectrophotometrically by coupling the hydrolysis of ATP to ADP to NADH oxidation (decrease in 340 nm absorbance) through the activities of pyruvate kinase (PK) and lactate dehydrogenase (LDH). Reactions contained 2 mmol/L phosphoenolpyruvate, 0.28 mmol/L NADH, 5 mmol/L $MgCl_2$, 1 mmol/L DTT, 15 μmol/L taxol, 0.7 μmol/L MT (preformed porcine microtubules; Cytoskeleton Inc.), 50 μmol/L ATP, 10 U/mL PK, and 10 U/mL LDH in 15 mmol/L PIPES buffer (pH 7.0). Reactions were initiated with a 20 nmol/L CENP-E addition (*Human*: 1-342; WT) at 30°C. The IC_{50} values were determined by a nonlinear, least squares fit of the data to the four-parameter dose–response curve equation (GraphPad Prism). PF-2771 kinesin biochemical selectivity toward other kinesins (Cytoskeleton Inc.) was tested in triplicate at both 1 and 10 μmol/L PF-2771 in a variant of the CENP-E enzymatic assays that had the following enzyme concentrations: 200 nmol/L chromokinesin motor domain, 200 nmol/L Eg5 motor domain, 226 nmol/L MCAK motor domain. PF-2771 biochemical mechanism was determined by measuring CENP-E enzymatic activity as a function of ATP and PF-2771 concentrations (0, 2.5, 5, 10, 20, 30, 45 nmol/L PF-2771; 1,000, 500, 250, 125, 62.5, 31.2, 15.6, 7.81, 3.90, 1.95, 0.977 μmol/L ATP).

Cell proliferation assays

PF-2771 was added to cells seeded in 96-well plates. The number of cells seeded (1,000–3,000) depended on growth characteristics of each cell type and normalized proliferation rates. Ten different concentrations of compound used were based on a half-log increment between 1 nmol/L and either 1 or 25 μmol/L. Cells were incubated at 37°C for 7 days before assessing viability with the CellTiter-Glo reagent (Promega). Untreated control cells were 80% to 90% confluent after 7 days of culture. Data were fitted into a sigmoidal curve-fitting program to calculate IC_{50} values.

Cellular ELISA assay for phosphorylation of histone H3-Ser_{10}

Cells were seeded in a 96-well plate in RPMI-1640 media supplemented with 10% fetal bovine serum (FBS)

and 1% penicillin-streptomycin at 37°C with 5% CO_2 until 80% to 90% confluence. Cells were then treated with PF-2771 at desired concentrations for 8 to 9 hours. Phospho-HH3-Ser_{10} was measured in triplicate using the PathScan phospho-HH3-Ser_{10} Sandwich ELISA Kit (Cell Signaling Technology). Data were exported and analyzed using a four-parameter IC_{50} (GraphPad Prism). In 20% FBS, PF-2771 is 48% unbound (free fraction).

Analysis of cell-cycle proteins in tumor cells

MDA-MB-468 cells were treated with PF-2771 (75 nmol/L) for 72 hours. Lysates (with protease and phosphatase inhibitors added) were resolved by NU-PAGE gels (Invitrogen), transferred to nitrocellulose membranes, and probed using antibodies for actin and cyclin B (Santa Cruz Biotechnology Inc.), AuroraB/AIM1, phospho-AuroraA(T288)/B(T232)/C(T198; Cell Signaling Technology; cat. #2914; 1:500 dilution), phospho-HH3-Ser_{10}, cleaved PARP (all from Cell Signaling Technology;), anti-phosphohistone-H2AX Ser139 (Millipore), securin (Abcam), anti-BubR1 (Bethyl Laboratories, Inc.), and 1:500 dilution anti-CENP-E (cat. #AKIN04-A, Cytoskeleton Inc.) overnight at 4°C. HRP-conjugated secondary antibodies (GE Healthcare) were incubated (2 hours, room temperature), detected using a chemiluminescent substrate (Pierce SuperSignal West Dura; Thermo Fisher Scientific), and imaged (Alpha Innotech imager; Cell Biosciences).

Flow cytometry

Analysis of cell-cycle distribution of cells was performed by flow cytometry. A MDA-MB-468 cell culture containing 1 to 2×10^6 cells was treated with the inhibitor (100 nmol/L) for 96 hours. The cells were fixated in 70% ethanol and stained with propidium iodine using the Cycletest Plus Kit (Becton Dickinson). The samples were analyzed on a Becton Dickinson FACSCalibur Instrument. The proportion of cells in G_1, S, G_2–M, aneuploidy or nongated (sub-G_1) was determined using CellQuest v. 2.0 software (Becton Dickinson).

In vivo tumor model studies

HCC1806 tumor cells (3×10^6) were implanted in the mammary fat pad of CB17/lcr.Cg-Prkdc^{scid}Lyst^{bg} female mice (Charles River Laboratories). PF-2771 was administered intraperitoneally (i.p.) to groups of 12 mice at 3, 10, and 30 mg/kg every day for 14 days and at 100 mg/kg every day for 4 days followed by 3 days off and then another 4-day cycle. Tumor volumes were recorded twice weekly by calipers with the final measurement taken 3 days after the last dose. Tumor growth inhibition (TGI) was calculated using the formula $100 \times (1 - \Delta T/\Delta C)$, where ΔT (treated) and ΔC (control) are the mean tumor volume changes between 1 day after the last dose and the first-day treatment. Time-to-progression endpoint and associated tumor growth delay determinations were calculated using median days to reach to two doublings of initial tumor size. Statistical comparisons were made using one-way ANOVA with Dunnett posttests. Other tumor models had similar methodology except where noted. PDX-AA1077 is a patient-derived xenograft model developed from tumor tissue from a triple-negative patient engrafted to the mammary glands of NSG female mice to create passage 1 tumor-bearing mice. Surgically resected tumor tissue was cut into 2- to 4-mm^3 fragments and subcutaneously implanted into the flank of SCID-bg mice (Charles River Laboratories). Mice with palpable tumors (passage 6) were randomized before dosing. An HCC1599 tumor cell line xenograft model was established from tumor fragments of established tumors and reimplanted into flank of female SCID mice. When average tumor size reached 250 mm^3, animals were randomized into five groups of 10 mice. Animals were treated with vehicle (daily dosing), 10 mg/kg docetaxel (once per week dosing), 25 mg/kg docetaxel (once per week dosing), 20 mg/kg paclitaxel (twice per week dosing), or 100 mg/kg of PF-2771 (every day, i.p.).

PK/PD analysis

Plasma drug concentrations and the pharmacodynamic endpoint (PD) tumor phospho-HH3-Ser_{10} responses in SCID mice bearing orthotopically implanted HCC1806 xenograft tumors (300–500 mm^3) were evaluated for vehicle or a single intraperitoneal dose of PF-2771. Tumors and plasma were collected at 1, 4, 8, 24, or 32 hours after dose (3 mice per time point). For plasma pharmacokinetics, mouse plasma was collected in heparinized vacutainers following intracardiac puncture. Plasma concentrations of PF-2771 were measured quantitatively with liquid chromatography–tandem mass spectrometry. The mass spectrometry was performed using electrospray ionization in the positive mode with multiple reaction monitoring (MRM). The plasma-free fraction of PF-2771 in SCID mouse plasma was measured using the equilibrium dialysis technique. Samples were extracted with 200 μL of acetonitrile containing an internal standard and analyzed by liquid chromatography—tandem mass spectrometry. The free fraction in plasma (f_u) was calculated by the equation $f_u = R_{buffer}/R_{plasma}$, where R_{buffer} and R_{plasma} represent the ratio of PF-2771. In mouse plasma, the free fraction of PF-2771 is calculated to be 0.022.

Results

CENP-E expression is highest in basal-like subtype among breast cancer patients

Gene expression in samples from 1,163 patients with breast cancer and 160 normal breast tissue samples were analyzed to identify dysregulated genes (public database; ref. 12). Although *CENPE* mRNA is significantly elevated across all segments of breast cancer relative to normal tissue, it is the highest in the basal-a subtype ($P = 2.22 \times 10^{-67}$ by two-tailed t test, fold change = 2.93; Fig. 1A). Analysis of breast cancer patient survival data reveals that the level of *CENPE* expression is strongly negatively correlated with disease-specific survival ($P = 3.68 \times 10^{-7}$ by log-rank test; Fig. 1B), indicating that CENP-E likely is involved in breast cancer biology. These patterns

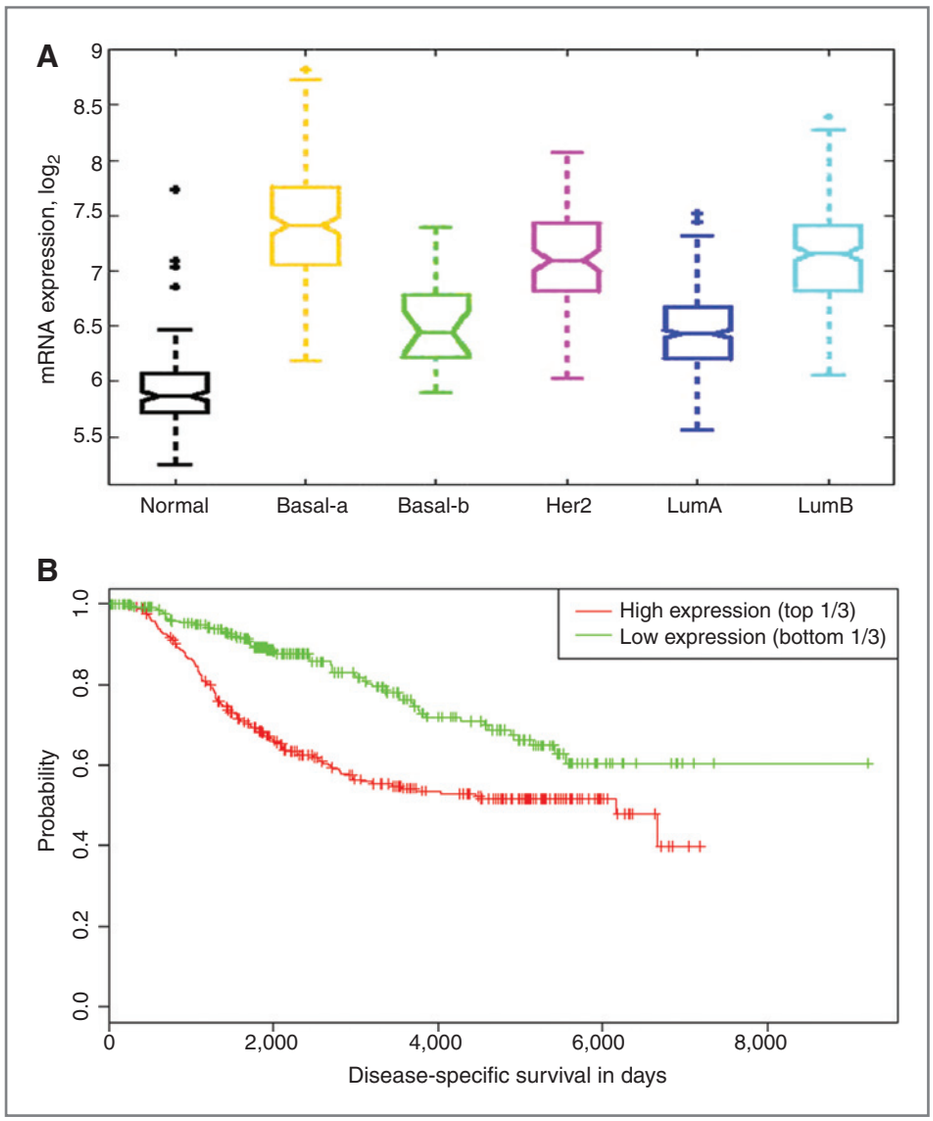

Figure 1. *CENPE* expression in breast tissues. A, genomic evaluation of CENP-E transcript level in breast cancer segments and adjacent normal tissue. B, CENP-E mRNA level is negatively related to disease-specific survival in breast cancer. Kaplan–Meier disease-specific survival analysis of patients with breast cancer stratified according to CENP-E expression.

are subsequently corroborated using an independent cohort from The Cancer Genome Atlas (TCGA; ref. 4). An evaluation of other mitotic regulators showed that their expression was also upregulated but the biology of CENP-E pointed to its potential driver role as a kinesin in cancer cells. To establish preclinical model systems, CENP-E protein expression was shown to be present in three basal-a breast cancer cell lines (HCC70, HCC1806, and MDA-MB-468). The response of CENP-E to spindle inhibitor treatment was evaluated in these cell lines (100 nmol/L docetaxel; 16 hours). CENP-E protein accumulates and the tumor cells undergo mitotic arrest (Fig. 2). Phosphorylation of BubR1 and HH3 were evaluated to provide mechanistic evidence for the activation of the SAC. Docetaxel treatment induced phosphorylation of serine residue 10 of histone H3 as well as BubR1 (supershifted bands in the SDS-PAGE; Fig. 2). Next, an inducible shRNA approach is used to characterize the consequences of CENP-E protein depletion on the *in vitro* viability of HCC1806 basal-like breast tumor cells. The CENP-E shRNA causes an 83% to 88% reduction of CENP-E mRNA 24 and 48 hours after transfection of cells (Supplementary Fig. S1A) and a greater than 90% reduction in CENP-E protein levels compared with the untransfected cells (Supplementary Fig. S1B). Upon doxycycline induction of specific CENP-E shRNA, only 20% of the HCC1806 tumor cells remain viable after 72 hours (Supplementary Fig. S1C). From this analysis, CENP-E is hypothesized to be critical in basal-a breast cancer cell biology.

PF-2771 is a potent, noncompetitive, selective inhibitor of CENP-E motor function

Because CENP-E is known to have both catalytic (ATPase motor activity) and noncatalytic functions (13), a more specific approach than shRNA knockdown is needed to study CENP-E ATPase motor function. To

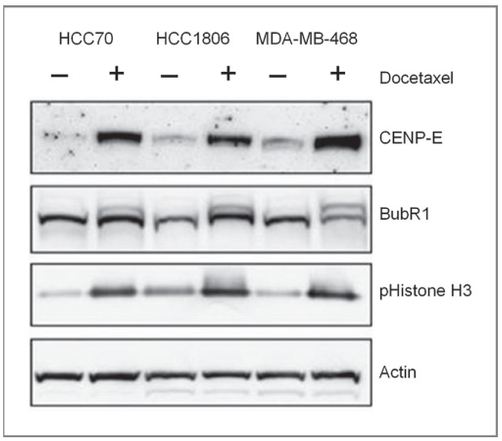

Figure 2. Evaluation of the effect of docetaxel treatment of basal tumor cell lines on SAC proteins. Docetaxel (100 nmol/L, 16 hours) induces CENP-E expression in breast tumor cell lines and pHH3, a molecular marker for the cell-cycle transition from metaphase to anaphase.

facilitate this analysis, the potent, selective inhibitor PF-2771 was synthesized, (Fig. 3, Supplementary Methods). This molecule inhibits CENP-E motor activity with an IC_{50} of 16.1 ± 1.2 nmol/L ($n = 18$) and a Hill slope of 0.94. Kinetic analysis of PF-2771 inhibition conducted as a function of ATP and PF-2771 concentrations is consistent with it being noncompetitive toward ATP (1/velocity vs. 1/[ATP] at varied [PF-2771] lines do not converge at the 1/v axis). PF-2771 does not inhibit the ATPase activities of highly related kinesins (0% inhibition of Eg5/KSP, chromokinesin, and MCAK at both 1 or 10 μmol/L PF-2771). PF-2771 is inactive toward a panel of 74 protein kinases (all <23% inhibition with 1 μmol/L PF-2771, <40% with 10 μmol/L PF-2771; Supplementary Table S1). The characterization of PF-2771 as a selective inhibitor of CENP-E motor activity enables its use as a probe of CENP-E biology in more complex systems.

PF-2771 is a specific CENP-E inhibitor critical to basal-like breast cancer tumor cell survival

Appropriate breast cancer contexts for studying PF-2771 were initially identified by measuring the sensitivity

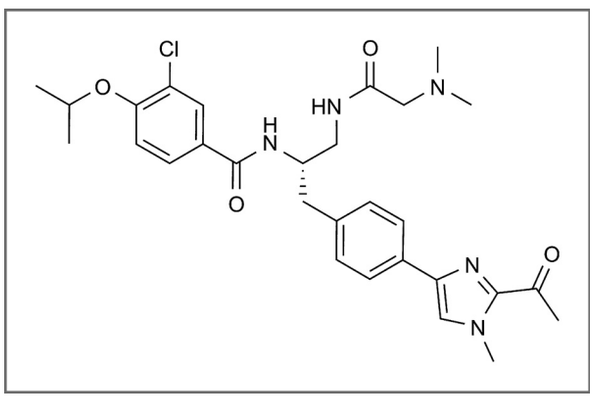

Figure 3. Chemical structure of PF-2771.

of breast cell lines to inhibition of CENP-E motor activity. The antiproliferative potency of PF-2771 (EC_{50} after 72 hours of treatment) was measured in 16 cell lines that span the following breast segments: normal breast epithelial cells, premalignant, basal-a, basal-b (claudin-low), luminal, and HER-2 positive (Fig. 4 and Supplementary Table S2). Cell line models lacking the receptors the define TNBC (HER-2, ER, and PR) encompass both basal-a and basal-b models. PF-2771 potency varies by three orders of magnitude across one cell line (0.01 to >10 μmol/L). All six cell lines sensitive to PF-2771 (EC_{50} < 0.1 μmol/L) are basal-like with five of these in the basal-a subset. In contrast, the normal and premalignant cell lines are not sensitive to PF-2771 treatment (EC_{50} > 5 μmol/L). These results suggest that CENP-E motor activity is necessary for breast cancer cell proliferation but dispensable for normal breast cell proliferation. Because PF-2771 is a potent inhibitor of basal-a tumor cell growth, two representative cell lines were selected for mechanistic analyses (MDA-MB-468 and HCC1806).

The molecular consequences of PF-2771 treatment in basal-a breast cancer cells were subsequently characterized to determine if they are consistent with CENP-E inhibition. CENP-E is known to be required for cell-cycle progression from metaphase to anaphase (13). Phosphorylation of the histone H3 Ser-10 (HH3-Ser_{10}) is used as a marker of CENP-E motor function because it is mediated by Aurora-B, coincident with chromosomal condensation, and decreases upon transition to anaphase (PF-2771 is not an Aurora-B inhibitor, Supplementary Table S1; ref. 14). The EC_{50} for the elevated phospho-HH3-Ser_{10} was determined to be 21 and 22 nmol/L in MDA-MB-468 and HCC1806 cells, respectively. The elevation of HH3-Ser_{10} phosphorylation is well correlated with inhibition of tumor cell proliferation (EC_{50}, 14–20 nmol/L) as well as inhibition of ATPase motor activity in a biochemical assay (IC_{50}, 16 nmol/L). A broader analysis of cellular effects of PF-2771 was undertaken by investigating other mitotic checkpoint proteins that are directly or indirectly associated with CENP-E (15, 16). PF-2771 treatment (75 nmol/L) of MDA-MB-468 tumor cells for 8 hours increases levels of phosphorylated BubR1, Aurora-B, securin, and cyclin B (Fig. 5). These results are consistent with PF-2771–dependent induction of mitotic arrest and the engagement of the SAC. At 24 hours after treatment of PF-2771, these markers of mitosis decrease, whereas increases in γH2AX (DNA damage) and cleaved PARP (apoptosis) proteins are observed.

The functional effects of PF-2771 treatment on tumor cells were characterized to better define the role of CENP-E motor activity in basal-like breast cancer biology. As CENP-E regulates the spindle assembly cell-cycle checkpoint, alterations in the cell-cycle profile are evaluated. Treatment of basal-a breast cancer tumor cells for 6 hours with 100 nmol/L PF-2771 causes an increase in the G_2–M cell population of basal-like tumor cells (43% MDA-MB-468 cells in G_2–M) relative to asynchronous, untreated cells (24% G_2–M; Supplementary Table S3). The time

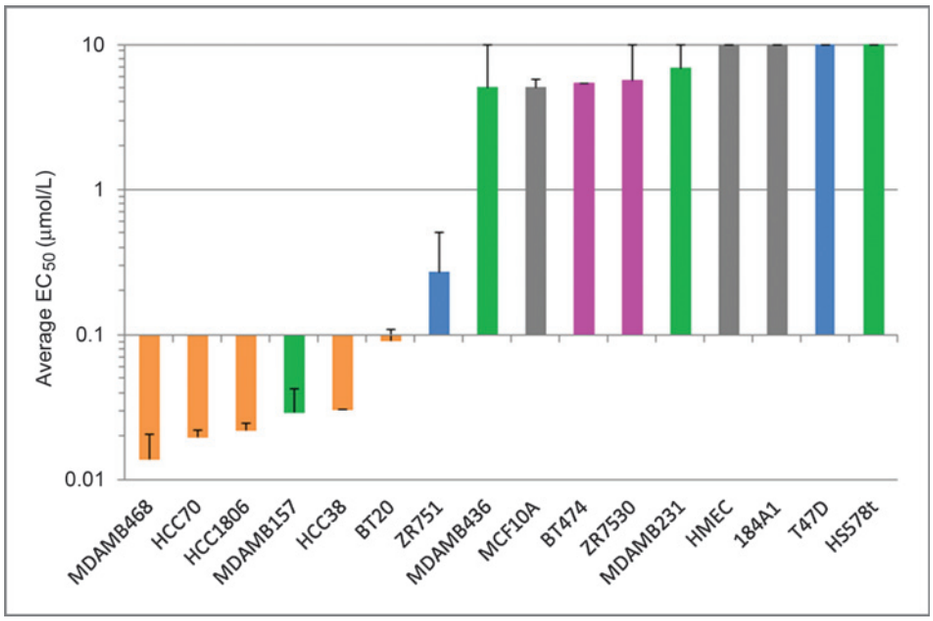

Figure 4. PF-2771 selectivity across a diverse panel of malignant and normal breast cell lines through the measurement of the inhibition of cell proliferation. The breast cell lines studied cover the following segments: normal/premalignant (gray), basal-a (orange), basal-b (claudin-low, green), HER-2 (magenta), and luminal (blue).

course of the cell-cycle effects caused by PF-2771 treatment shows a rapid accumulation of cells at the G_2–M stage followed by a large increase in the sub-G_0 population (Supplementary Table S3). It should be noted that normal breast cells have a small G_2–M population (G_0–G_1 ~ 85%; ref. 17). After 96 hours, the sub-G_1 cell population is 23% compared with 5% in control cells; consistent with onset of apoptosis following mitotic delay (Supplementary Table S3). Because this cell-cycle phenotype is not exclusive to CENP-E, other more specific functional effects were investigated such as chromosome congression—a process necessary for the establishment of bidirectional chromosome/kinetochore attachments before the onset of anaphase (18). Exposure of tumor cells to a *bona fide* CENP-E inhibitor should result in mitotic delay due to the presence of uncongressed chromosomes. Basal-a tumor cells (MDA-MB-468) were engineered to constitutively express the fluorescent reporter histone-2B green fluorescent protein (H2B-GFP) to follow chromosome dynamics through fluorescent live-cell video microscopy (Fig. 6). Vehicle-treated cells complete mitosis in approximately 1 hour as measured by nuclear envelope breakdown to onset of cytokinesis. In contrast, 100 nmol/L PF-2771–treated tumor cells display a delayed metaphase–anaphase transition (~3 hours) followed by either mitotic apoptosis or mitotic slippage with subsequent apoptosis (Fig. 6). In contrast, PF-2771 does not exhibit the characteristic phenotype associated with inhibition of the related kinesin EG5/KSP. EG5/KSP inhibitors (e.g., ispinesib) trigger the formation of monopolar spindles (19), a phenotype that is not observed in tumor cells exposed to PF-2771 (Supplementary Fig. S2). A chromosome congression defect is observed in the PF-2771–treated cells because chromosomes remained distant from the metaphase plate for at least twice as long as vehicle-treated cells. Taken together, PF-2771 modulates CENP-E dependent molecular markers in basal-like breast cancer cells and has the functional hallmarks of a selective CENP-E inhibitor.

Cellular sensitivity to inhibition of CENP-E motor function is correlated with degree of CIN

An evaluation of the relationship between CENP-E expression and PF-2771 response finds that there is no statistically significant difference in CENP-E mRNA levels between sensitive and resistant cell lines ($P = 0.52$ by two-tailed t test). As SAC defects are found in cancer cells with high levels of CIN (20, 21), a plausible hypothesis is that tumors with this phenotype are more reliant on genes that regulate the SAC and therefore sensitive to inhibition of CENP-E motor function. Furthermore, high CIN tumor cells are enriched for cells with merotelic chromosomal attachments (lagging chromosomes; ref. 22). A CIN index measurement is devised to quantify the overall level of DNA copy-number change in various breast cell lines. Cell lines are divided into sensitive and resistant groups based on response to PF-2771 (EC_{50} cutoff was 0.1 μmol/L). Tumor cell lines sensitive to PF-2771 have a much higher CIN index score than resistant ones ($P = 0.022$ by two-tailed t test), suggesting that breast cancer tumors with elevated chromosomal instability are likely to benefit from CENP-E–targeted therapy.

Inhibition of CENP-E is efficacious in tumor cell line and patient-derived basal-like breast cancer tumor models

Three tumor models are used to investigate the role of CENP-E in basal-a breast cancer—HCC1806 basal-a tumor xenograft, PDZ-AA1077 (basal-like) patient-derived TNBC breast cancer model, and HCC1599

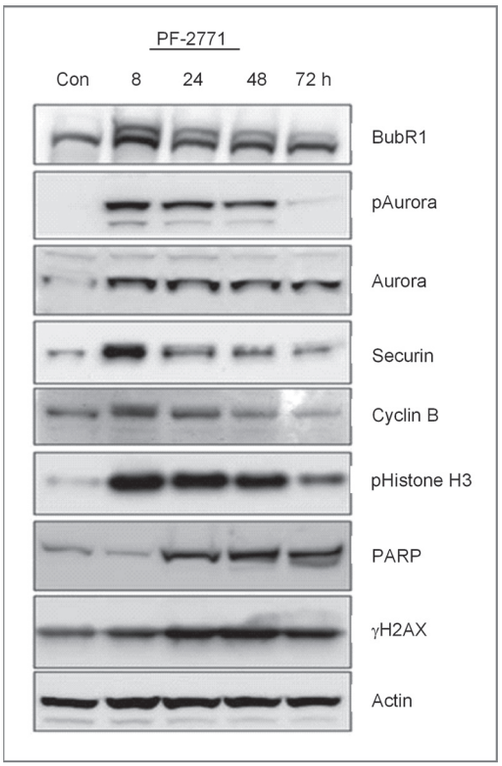

Figure 5. PF-2771 regulates cell-cycle markers in MDA-MB-468 TNBC tumor cells expected to be CENP-E dependent and induces cell-cycle arrest. The expression of an array of proteins was analyzed by Western blot analyses of lysates from MDA-MB-468 cells treated with 75 nmol/L PF-2771 for up to 72 hours.

(basal-a) taxane-resistant tumor xenograft model. TGI of the HCC1806 model is observed to be 24% at 30 mg/kg ($P = 0.046$ by t test) and 62% regression at 100 mg/kg ($P = 9.4 \times 10^{-8}$ by t test) measured after 14 days of PF-2771 treatment (Fig. 7A). Animals treated with PF-2771 exhibited no significant body weight loss (<10%; Supplementary Fig. S3) and displayed normal grooming and other behaviors. Single-dose treatment with 100 mg/kg of PF-2771 results in significant elevation (up to 6-fold increase) of phospho-HH3-Ser_{10}, which was sustained up to 24 hours (Fig. 7B).

To better define the role of CENP-E inhibition in the HCC1806 xenograft model, we quantified the temporal relationship between plasma concentrations of PF-2771, a pharmacodynamic marker for CENP-E inhibition, and subsequent TGI. Phosphorylation of histone H3 residue Ser-10 is evaluated because it is well correlated with other SAC functions in cellular studies of PF-2771 and is a robust marker of mitotic arrest and SAC activation (14). A detailed description of the mathematical PK/PD modeling methods and results can be found in the Supplementary Methods. Briefly, tumor cell growth and kill rates in the mathematical model represent the overall growth and death rates of cells comprising the tumor volume in the mouse (Supplementary Fig. S4, right). The growth rate slows as the tumor increases in volume as seen in the control group (Supplementary Fig. S4, center). The kill rate is a function of the concentration of the CENP-E inhibitor in the system, consistent with the hypothesis that inhibition of CENP-E motor function induces apoptosis. The *in vivo* EC_{50} of PF-2771 for phospho-HH3-Ser_{10} elevation is estimated by the mathematical model to be 4.1 nmol/L (free-drug concentration). The elevated phosphoHH3-Ser_{10} levels are responsive in a predicable fashion, consistent with a standard Hill function (Supplementary Fig. S4). The *in vivo* EC_{50} value is consistent with the *in vitro* cellular IC_{50} (11 nmol/L) in the HCC1806 cell line as well as the biochemical potency (IC_{50}, 16 nmol/L). The modeling results also highlight the inability of lower PF-2771 doses (3, 10, and 30 mg/kg) to increase the kill rate and sustain it at an adequate level to significantly slow (or regress) tumor growth. However, in the 100 mg/kg group, a significantly elevated kill rate is sustained during dosing, thus overpowering the growth rate and causing tumor regression. These results establish a strong correlation between inhibition of CENP-E motor function and efficacy in basal-a breast cancer.

To study CENP-E motor function in a model that better reflects breast cancer patient biology, PF-2771 was evaluated in an patient-derived TNBC model that is generated by directly engrafting primary human tumor tissue into murine mammary tissue (PDX-AA1077; ref. 23). By genome-wide gene expression profiling, we confirm that the xenograft tumor is from basal-a breast cancer. The Pearson correlation with intrinsic centroids for PDZ-AA1077 are as follows: 0.2067 (basal-like), −0.0269 (Her-2), −0.1437 (luminal-a), −0.0665 (luminal-b), and −0.0165 (normal-like). SCID mice bearing AA1077 mammary tumors treated with a PF-2771 dose known to potently inhibit CENP-E motor function (100 mg/kg every day i.p.) exhibit tumor regression (99.97%; Fig. 8A). This finding provides additional support that inhibition of CENP-E motor function could be efficacious in a selected patient population.

PF-2771 was used to evaluate CENP-E motor function inhibition relative to mitotic spindle inhibitors (paclitaxel and docetaxel) in the HCC1599 basal-a tumor model. At clinically relevant murine doses (24), paclitaxel (20 mg/kg twice weekly) and docetaxel (25 mg/kg/week) had moderate efficacy in the HCC1599 model (paclitaxel TGI 78%, $P = 2.63 \times 10^{-8}$ by t test; docetaxel 76% TGI, $P = 2.74 \times 10^{-8}$ by t test). As such, the HCC1599 model is less responsive to taxane treatment compared with other breast cancer models. In contrast, at an effective PF-2771 dose (100 mg/kg every day), substantial tumor regression is observed in this model (64% regression, $P = 7.63 \times 10^{-9}$ by t test; Fig. 8B). These results suggest that a CENP-E inhibitor could be more effective than traditional chemotherapies for a subset of patients and that CENP-E inhibitors may be mechanistically distinct from spindle poisons.

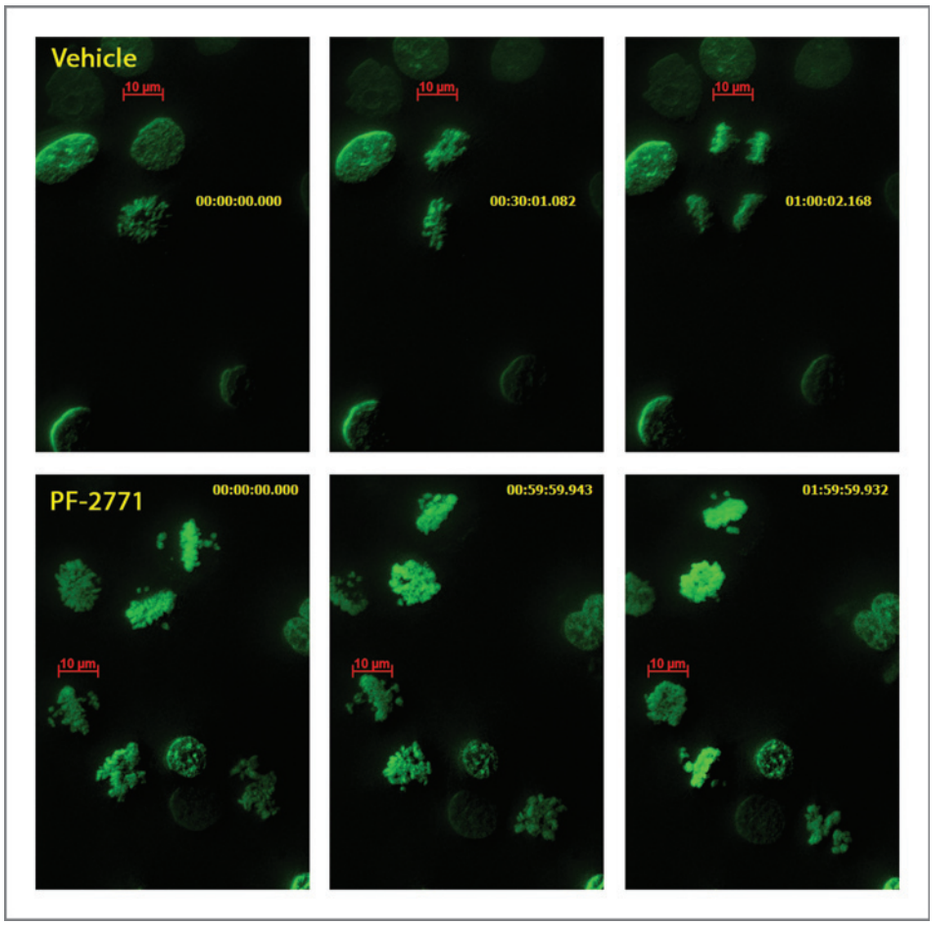

Figure 6. PF-2771 causes a chromosomal congression defect. MDA-MB-468 cells engineered to stably express H2B-GFP were subject to live-cell imaging. Representative cell images from the 15-hour treatment are as follows: vehicle 0.1% DMSO vehicle at 0-, 30-, and 60-minute time points (top); treatment with 100 nmol/L PF-2771 at 0-, 60-, and 120-minute time points (bottom).

Discussion

A major paradigm change in the treatment of patients with cancer is under way—matching a targeted therapy to a molecular event essential to a specific tumor biology. When this occurs, profound clinical benefit is realized as observed with imatinib in BCR-ABL–dependent leukemia, vemurafenib and dabrafenib in Braf V600E-driven melanoma, and crizotinib in EML4–ALK–positive lung cancer. Through a combination of genomic and chemical biologic approaches, we characterize the kinesin CENP-E as critical to basal-a, TNBC. To date, CENP-E–directed therapies have not been broadly pursued, in part, due to the notion that cell-cycle inhibitors will be similar to classic cytotoxic agents. However, recent clinical findings on the cell-cycle checkpoint inhibitor palbociclib (CDK4/6 inhibitor) demonstrate that this type of intervention can be well tolerated with profound therapeutic benefit (25).

CENP-E is a member of the kinesin super family of 650 motor proteins that use the energy from ATP hydrolysis to transport cellular cargos (11, 26). CENP-E has an N-terminal catalytic motor domain, a discontinuous α-helical coiled-coil stalk domain, and a C-terminal ATP-independent microtubule-binding domain (10, 11). Depletion of CENP-E leads to mitotic arrest due to the presence of unaligned chromosomes (27). We show that CENP-E accumulates in basal-a breast cancer cells following taxane treatment. Previous studies show that CENP-E protein turnover occurs after the completion of mitosis (11). As taxanes are known to induce a mitotic arrest, lysates made from taxane-treated cells should, therefore, show an enhanced amount of CENP-E protein. Evidence for the therapeutic benefit of inhibiting CENP-E comes from previous studies of mice with one CENP-E allele (heterozygous for CENP-E), which exhibit decreased incidence of tumors induced by carcinogens or from the heterozygous deletion of the tumor suppressor $p19^{ARF}$ (28). A recent study reports that CENP-E protein has cellular activities in addition to its motor function (29). Therefore, eliminating or knocking down the expression of an entire CENP-E protein provides valuable information but lacks the resolution to characterize specific protein functions.

Unlike other therapeutic targets (e.g., protein kinases), there are a limited number of kinesin inhibitors and even fewer CENP-E inhibitors available to investigate their biologic roles in cancer. UA62784 has been reported to be a CENP-E inhibitor (30), yet subsequent mechanistic studies show that UA62784 does not exert its cellular activity by inhibiting CENP-E but by binding microtubules tightly (31). GSK923295 is an allosteric inhibitor of CENP-E, which advanced to a phase I clinical trial of

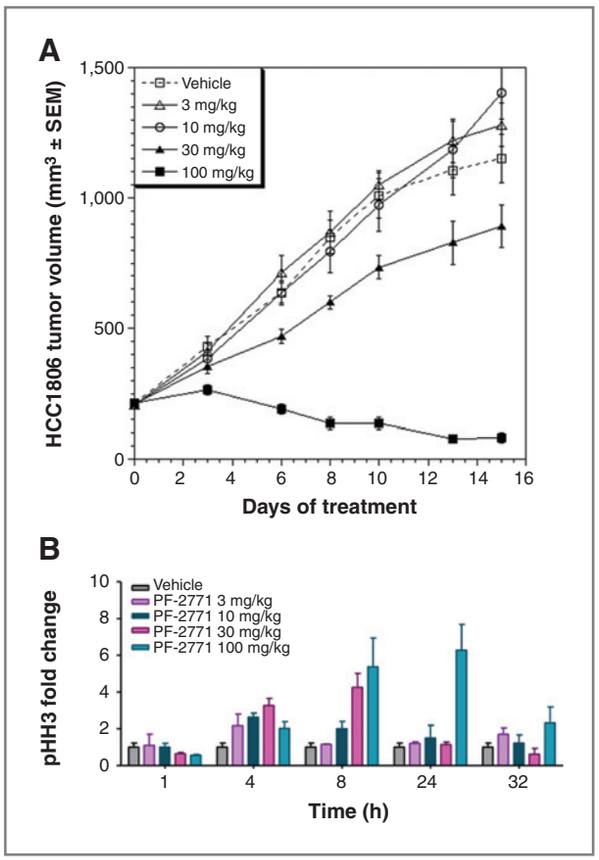

Figure 7. Pharmacodynamic profile and *in vivo* antitumor activity of PF-2771 in HCC1806 xenograft model. A, SCID mice were treated with vehicle (□), 3 (Δ), 10 (○), 30 (▲) mg/kg of PF-2771 once daily for 14 days. SCID mice were treated with 100 mg/kg (■) of PF-2771 with the following schedule: once daily or with vehicle for 4 days, 3-day dosing holiday, another 4-day dosing cycle. Thirty mg/kg resulted in 27% TGI ($P = 0.046$) and 100 mg/kg caused 62% tumor regression ($P = 9.5 \times 10^{-8}$). Data are presented as mean ± SE of 12 mice in each group. B, SCID mice were treated with 3, 10, 30, and 100 mg/kg doses of PF-2771 or with vehicle. Tumor and plasma were collected at 1, 4, 8, 24, and 32 hours after dose. Phospho-HH3-Ser_{10} levels were assessed by ELISA assay using tumor lysates.

unselected patients with cancer with refractory disease (27, 32). Although the therapy was well tolerated, the utility of this agent in an unselected patient population was modest with a single partial response reported. This may be due to either insufficient pharmacodynamic modulation of CENP-E or the selection of an incorrect patient population. A third CENP-E inhibitor (syntelin) has been reported to have moderate potency (IC_{50}, 160 nmol/L), but has only been studied in cellular systems (33). As such, there is a need for a selective CENP-E inhibitor with a well-defined mechanism of action and sufficient pharmaceutical properties to define a patient selection hypothesis to test in the clinic.

The inhibitor PF-2771 was developed to investigate the role of CENP-E motor function in TNBC. Biochemical analysis of PF-2771 is consistent with it being a potent, selective inhibitor of the CENP-E motor function. A detailed evaluation of PF-2771 in basal-a breast cancer tumor cells is consistent with specific CENP-E inhibition and therefore useful for studying CENP-E motor function in tumor models. Because tumor cell line–derived tumor models do not fully capture disease biology, in part, because they are adapted to grow in two-dimensional

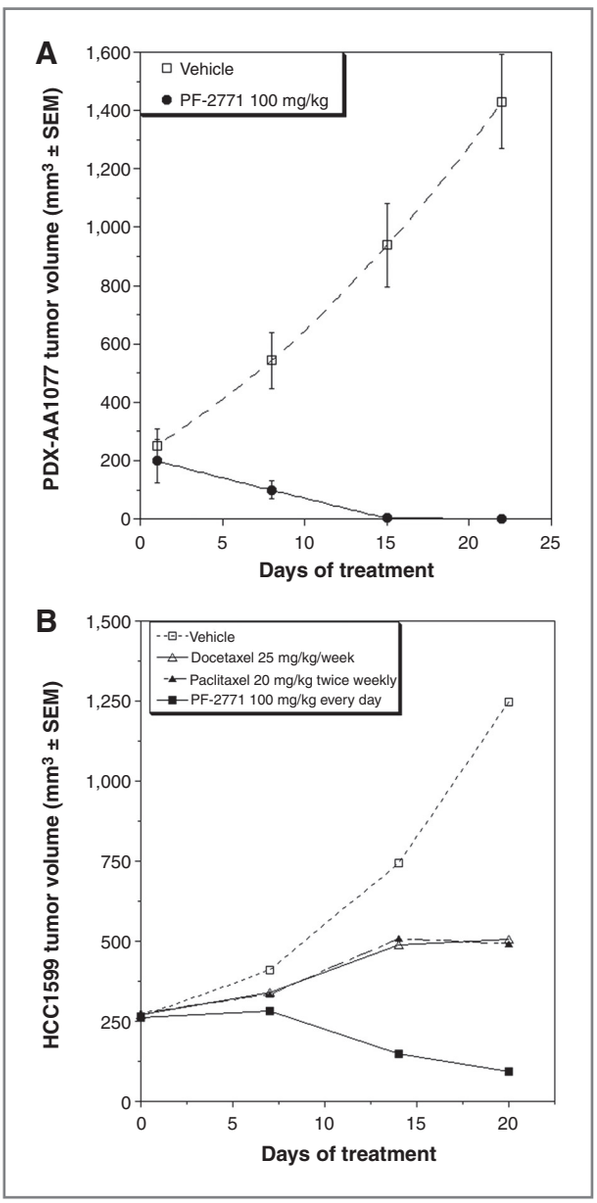

Figure 8. A, evaluation of PF-2771 in a patient-derived, basal-a breast cancer xenograft model (PDX-AA1077). SCID mice (7 mice per group) were treated with 100 mg/kg PF-2771 i.p. every day (●) or vehicle (□) for 21 days with the data presented as mean ± SEM. B, HCC1599 basal-like breast cancer tumor model evaluation of PF-2771 (■) efficacy relative to vehicle (□), docetaxel (△), and paclitaxel (▲). Dosing was as follows: 25 mg/kg/week docetaxel, 20 mg/kg twice weekly paclitaxel, and 100 mg/kg every day PF-2771. Data are presented as mean ± SE of 10 mice in each group.

(2D) culture, we evaluated PF-2771 in a patient-derived, basal-a tumor model. This approach is emerging as a superior method to predict clinical efficacy (34). At PF-2771 doses expected to inhibit CENP-E motor function, complete tumor regression in the patient-derived model is observed, which predicts a likelihood of clinical benefit for this segment of breast cancer. In addition, PF-2771 demonstrates better efficacy as compared with taxanes in another triple-negative, basal-a breast tumor model (HCC1599), which we show to be partially insensitive to taxane treatment. These findings provide evidence that abrogating the SAC by inhibiting CENP-E motor activity may be an effective treatment for patients with basal-a TNBC.

There is significant pressure to accelerate the discovery of new cancer therapies by conducting more effective clinical trials. Central to this task is determining if inhibition of the intended drug target is effective in managing disease—does modulation of a therapeutic target-specific molecular pharmacodynamic biomarker correlate with efficacy? This detailed analysis has been lacking for both preclinical and clinical studies of CENP-E inhibitors. Previously published findings show a lack of efficacy of a different CENP-E inhibitor (GSK923295) in the MX-1 breast cancer model (no regression observed in animals dosed with either 62.5 mg/kg or 125 mg/kg; ref. 27). In this study, one does not know if an insensitive patient population (tumor model) was selected or if the inhibitor failed to inhibit CENP-E in the tumor. With the preclinical studies of PF-2771, both of these variables are well understood. Interestingly, GSK932295 is reported to be selectively potent toward basal-b tumor cells (AACR poster, April 2009) and induces MX-1 cell arrest briefly without subsequent apoptosis (AACR-NCI-EORTC poster, October 2007)—strikingly different findings than we report for PF-2771. Inhibition of CENP-E motor function by PF-2771 resulted in tumor regression in a HCC1806 basal-like breast cancer xenograft tumor model (also HCC70, data not shown). Importantly, the tumor regression driven by PF-2771 occurs concurrently with cell-cycle arrest as evidenced by dose-dependent elevation of phospho-HH3-Ser_{10} levels. Detailed PK/PD modeling demonstrated that PF-2771–dependent TGI/regression is highly correlated with antimitotic properties expected for CENP-E inhibition and, thus, suggests the basis of efficacy.

Analysis of PF-2771 antiproliferative cell potency revealed a paradox that cell line sensitivity to PF-2771 is poorly correlated with CENP-E gene expression. This relationship can be expected to be complicated because PF-2771 only inhibits the CENP-E motor function and spares the motor-independent functions (13). Nonetheless, there is a wide range of PF-2771 activities observed from potent inhibition of basal-a breast cancer cell to insensitivity in premalignant cells. The strong correlation observed between PF-2771 cell line sensitivity and CIN is interesting and potentially useful. When reevaluating cell line sensitivity to PF-2771, the contribution of CIN to the disease segment may be a critical attribute. For example, basal-a breast cancer is known to have high genomic instability (35). Although genomic instability is a hallmark of human cancer (36), tumor genomes vary considerably in the level of instability that they harbor (37) and the mechanisms by which they become unstable (35). Importantly, patients with highly unstable tumor genomes often have poorer prognosis (37–40). The subset of genomic instability known as CIN is caused by multiple mechanisms such as (i) faulty sister chromatid cohesion, (ii) defective centrosome duplication, (iii) telomere dysfunction, (iv) overly stable attachments of microtubules to chromosomes, and (v) hyperactive or hypoactive SAC (22). Recent studies of reduced CENP-E through the loss of an allele, CENP-E (+/−), report that tumor cells that do not arise from CIN are unaffected by CENP-E–dependent chromosomal missegregation (41). Our pharmacologic studies coupled with these genetic studies indicate that tumor cells with high CIN may have "induced essentiality" of CENP-E (related to the genetic concept of synthetic-lethal; refs. 42, 43). The preferential cytotoxicity of PF-2771 to tumor cells with high CIN relative could be because these cells rely on CENP-E to accommodate the chromosomal instability. An alternative hypothesis (not mutually exclusive) is that CENP-E supports a tumor's use of CIN as a cellular mechanism to generate tumor genomic diversity, a trait that would favor the emergence of drug resistance. The clinical utility of induced essentiality has been demonstrated with related DNA damage repair machinery. Inhibiting the single-strand DNA repair enzyme PARP in tumors with mutations in the DNA damage tumor-suppressor BRCA1/2 is proving to be clinically effective (43). Taken together, these findings indicate that basal-a TNBC and other patient populations with chromosomal instability (44, 45) may benefit from a CENP-E–targeted therapy.

PF-2771 is useful in evaluating potential safety liabilities of inhibiting CENP-E, a concern with inhibiting any cell cycle–related enzyme. We find evidence that CENP-E inhibition could be well tolerated in patients. Normal breast cells are not affected by PF-2771, which supports the hypothesis that inhibiting CENP-E will be synthetic lethal to tumor cells. Multiple *in vivo* studies show that PF-2771 is well tolerated. In a recent phase I clinical study on a different CENP-E inhibitor, a well-known taxane adverse effect (neuropathy) is not listed among the adverse events (27). As such, CENP-E inhibitors have the potential to be better tolerated than taxanes and possibly easier to use in combination with other cancer therapies. Our comprehensive analysis of CENP-E supports the hypothesis that this mitotic kinesin is a therapeutic target for the treatment of the triple-negative/basal-a segment of breast cancer with possibilities in other CIN-dependent cancers.

Disclosure of Potential Conflicts of Interest

P. Wells has ownership interest (including patents) in Pfizer Inc. No potential conflicts of interest were disclosed by the other authors.

Authors' Contributions

Conception and design: P.-P. Kung, R. Martinez, Z. Zhu, M. Zager, A. Blasina, O. Guicherit, M. Cui, Z. Huang, B.W. Murray

Development of methodology: R. Martinez, Z. Zhu, A. Blasina, I. Rymer, J. Hallin, M. Xu, P. Wells, J. Fan, O. Guicherit, B. Huang, Z. Huang, B.W. Murray

Acquisition of data (provided animals, acquired and managed patients, provided facilities, etc.): R. Martinez, I. Rymer, J. Hallin, M. Xu, C. Carroll, J. Chionis, P. Wells, K. Kozminski, J. Fan, M. Cui, C. Liu, Z. Huang, A. Sistla, B.W. Murray

Analysis and interpretation of data (e.g., statistical analysis, biostatistics, computational analysis): R. Martinez, Z. Zhu, M. Zager, A. Blasina, I. Rymer, M. Xu, C. Carroll, P. Wells, K. Kozminski, J. Fan, O. Guicherit, M. Cui, C. Liu, Z. Huang, B.W. Murray

Writing, review, and/or revision of the manuscript: P.-P. Kung, R. Martinez, Z. Zhu, M. Zager, J. Hallin, P. Wells, B. Huang, M. Cui, J. Yang, B.W. Murray

Administrative, technical, or material support (i.e., reporting or organizing data, constructing databases): A. Blasina, I. Rymer, C. Liu

Study supervision: A. Blasina, O. Guicherit, Z. Huang, J. Yang, B.W. Murray

Acknowledgments

The authors thank the assistance of Dr. Jeff Koup in the PK/PD modeling work and analysis. The authors also thank Drs. Martin Wythes, Martin Edwards, Robert Kania, Paul Richardson, Norm Greenberg, Gary Li, Gerrit Los, Stephan Grant, and Valeria Fantin for helpful discussions.

Grant Support

All work in this study was sponsored by Pfizer.

The costs of publication of this article were defrayed in part by the payment of page charges. This article must therefore be hereby marked *advertisement* in accordance with 18 U.S.C. Section 1734 solely to indicate this fact.

Received January 28, 2014; revised May 9, 2014; accepted May 29, 2014; published OnlineFirst June 30, 2014.

References

1. Fisher B, Redmond C, Brown A, Wickerham DL, Wolmark N, Allegra J, et al. Influence of tumor estrogen and progesterone receptor levels on the response to tamoxifen and chemotherapy in primary breast cancer. J Clin Oncol 1983;1:227–41.
2. Slamon DJ, Leyland-Jones B, Shak S, Fuchs H, Paton V, Bajamonde A, et al. Use of chemotherapy plus a monoclonal antibody against HER2 for metastatic breast cancer that overexpresses HER2. N Engl J Med 2001;344:783–92.
3. Boyle P. Triple-negative breast cancer: epidemiological considerations and recommendations. Ann Oncol 2012;23(Suppl 6): vi7–12.
4. Cancer Genome Atlas N. Comprehensive molecular portraits of human breast tumours. Nature 2012;490:61–70.
5. Dent R, Trudeau M, Pritchard KI, Hanna WM, Kahn HK, Sawka CA, et al. Triple-negative breast cancer: clinical features and patterns of recurrence. Clin Cancer Res 2007;13:4429–34.
6. Ellis P, Barrett-Lee P, Johnson L, Cameron D, Wardley A, O'Reilly S, et al. Sequential docetaxel as adjuvant chemotherapy for early breast cancer (TACT): an open-label, phase III, randomised controlled trial. Lancet 2009;373:1681–92.
7. Hilkens PH, Verweij J, Stoter G, Vecht CJ, van Putten WL, van den Bent MJ. Peripheral neurotoxicity induced by docetaxel. Neurology 1996; 46:104–8.
8. New PZ, Jackson CE, Rinaldi D, Burris H, Barohn RJ. Peripheral neuropathy secondary to docetaxel (Taxotere). Neurology 1996;46: 108–11.
9. Hauf S. The spindle assembly checkpoint: progress and persistent puzzles. Biochem Soc Trans 2013;41:1755–60.
10. Yen TJ, Compton DA, Wise D, Zinkowski RP, Brinkley BR, Earnshaw WC, et al. CENP-E, a novel human centromere-associated protein required for progression from metaphase to anaphase. EMBO J 1991;10:1245–54.
11. Yen TJ, Li G, Schaar BT, Szilak I, Cleveland DW. CENP-E is a putative kinetochore motor that accumulates just before mitosis. Nature 1992;359:536–9.
12. Curtis C, Shah SP, Chin SF, Turashvili G, Rueda OM, Dunning MJ, et al. The genomic and transcriptomic architecture of 2,000 breast tumours reveals novel subgroups. Nature 2012;486:346–52.
13. Rath O, Kozielski F. Kinesins and cancer. Nat Rev Cancer 2012;12: 527–39.
14. Sawicka A, Seiser C. Histone H3 phosphorylation—a versatile chromatin modification for different occasions. Biochimie 2012;94:2193–201.
15. Wood KW, Chua P, Sutton D, Jackson JR. Centromere-associated protein E: a motor that puts the brakes on the mitotic checkpoint. Clin Cancer Res 2008;14:7588–92.
16. Guo Y, Kim C, Ahmad S, Zhang J, Mao Y. CENP-E–dependent BubR1 autophosphorylation enhances chromosome alignment and the mitotic checkpoint. J Cell Biol 2012;198:205–17.
17. Ross JS, Linette GP, Stec J, Ross MS, Anwar S, Boguniewicz A. DNA ploidy and cell cycle analysis in breast cancer. Am J Clin Pathol 2003;120(Suppl):S72–84.
18. Brown KD, Wood KW, Cleveland DW. The kinesin-like protein CENP-E is kinetochore-associated throughout poleward chromosome segregation during anaphase-A. J Cell Sci 1996;109(Pt 5): 961–9.
19. Kapoor TM, Mayer TU, Coughlin ML, Mitchison TJ. Probing spindle assembly mechanisms with monastrol, a small molecule inhibitor of the mitotic kinesin, Eg5. J Cell Biol 2000;150: 975–88.
20. Schvartzman JM, Sotillo R, Benezra R. Mitotic chromosomal instability and cancer: mouse modelling of the human disease. Nat Rev Cancer 2010;10:102–15.
21. Yoon DS, Wersto RP, Zhou W, Chrest FJ, Garrett ES, Kwon TK, et al. Variable levels of chromosomal instability and mitotic spindle checkpoint defects in breast cancer. Am J Path 2002;161: 391–7.
22. Bakhoum SF, Compton DA. Chromosomal instability and cancer: a complex relationship with therapeutic potential. J Clin Invest 2012; 122:1138–43.
23. Zhang CC, Yan Z, Zong Q, Fang DD, Painter C, Zhang Q, et al. Synergistic effect of the gamma-secretase inhibitor PF-03084014 and docetaxel in breast cancer models. Stem Cell Transl Med 2013;2: 233–42.
24. Sparreboom A, van Tellingen O, Nooijen WJ, Beijnen JH. Preclinical pharmacokinetics of paclitaxel and docetaxel. Anticancer Drugs 1998;9:1–17.
25. Guha M. Blockbuster dreams for Pfizer's CDK inhibitor. Nat Biotechnol 2013;31:187.
26. Kim Y, Heuser JE, Waterman CM, Cleveland DW. CENP-E combines a slow, processive motor and a flexible coiled coil to produce an essential motile kinetochore tether. J Cell Biol 2008;181: 411–9.
27. Wood KW, Lad L, Luo L, Qian X, Knight SD, Nevins N, et al. Antitumor activity of an allosteric inhibitor of centromere-associated protein-E. Proc Natl Acad Sci U S A 2010;107:5839–44.
28. Weaver BA, Silk AD, Montagna C, Verdier-Pinard P, Cleveland DW. Aneuploidy acts both oncogenically and as a tumor suppressor. Cancer Cell 2007;11:25–36.
29. Maiato H, Logarinho E. Mitotic-dependent and -independent roles of CENP-E at kinetochores: the cautionary tale of UA62784. Chem Biol 2011;18:679–80.
30. Henderson MC, Shaw YJ, Wang H, Han H, Hurley LH, Flynn G, et al. UA62784, a novel inhibitor of centromere protein E kinesin-like protein. Mol Cancer Ther 2009;8:36–44.
31. Tcherniuk S, Deshayes S, Sarli V, Divita G, Abrieu A. UA62784 is a cytotoxic inhibitor of microtubules, not CENP-E. Chem Biol 2011;18: 631–41.

32. Chung V, Heath EI, Schelman WR, Johnson BM, Kirby LC, Lynch KM, et al. First-time-in-human study of GSK923295, a novel antimitotic inhibitor of centromere-associated protein E (CENP-E), in patients with refractory cancer. Cancer Chemother Pharmacol 2012;69:733–41.
33. Ding X, Yan F, Yao P, Yang Z, Wan W, Wang X, et al. Probing CENP-E function in chromosome dynamics using small molecule inhibitor syntelin. Cell Res 2010;20:1386–9.
34. Siolas D, Hannon GJ. Patient-derived tumor xenografts: transforming clinical samples into mouse models. Cancer Res 2013;73:5315–9.
35. Kwei KA, Kung Y, Salari K, Holcomb IN, Pollack JR. Genomic instability in breast cancer: pathogenesis and clinical implications. Mol Oncol 2010;4:255–66.
36. Negrini S, Gorgoulis VG, Halazonetis TD. Genomic instability—an evolving hallmark of cancer. Nat Rev Mol Cell Biol 2010;11:220–8.
37. Sheltzer JM. A transcriptional and metabolic signature of primary aneuploidy is present in chromosomally unstable cancer cells and informs clinical prognosis. Cancer Res 2013;73:6401–12.
38. Auer G, Eriksson E, Azavedo E, Caspersson T, Wallgren A. Prognostic significance of nuclear DNA content in mammary adenocarcinomas in humans. Cancer Res 1984;44:394–6.
39. Carter SL, Eklund AC, Kohane IS, Harris LN, Szallasi Z. A signature of chromosomal instability inferred from gene expression profiles predicts clinical outcome in multiple human cancers. Nat Genet 2006;38:1043–8.
40. Mettu RK, Wan YW, Habermann JK, Ried T, Guo NL. A 12-gene genomic instability signature predicts clinical outcomes in multiple cancer types. Int J Biol Markers 2010;25:219–28.
41. Silk AD, Zasadil LM, Holland AJ, Vitre B, Cleveland DW, Weaver BA. Chromosome missegregation rate predicts whether aneuploidy will promote or suppress tumors. Proc Natl Acad Sci U S A. 2013;110:E4134–41.
42. Hartwell LH, Szankasi P, Roberts CJ, Murray AW, Friend SH. Integrating genetic approaches into the discovery of anticancer drugs. Science 1997;278:1064–8.
43. Nijman SM, Friend SH. Cancer. Potential of the synthetic lethality principle. Science 2013;342:809–11.
44. Duensing S, Munger K. Mechanisms of genomic instability in human cancer: insights from studies with human papillomavirus oncoproteins. Int J Cancer J 2004;109:157–62.
45. Pikor L, Thu K, Vucic E, Lam W. The detection and implication of genome instability in cancer. Cancer Metastasis Rev 2013;32:341–52.